

Investigation, analysis and comparison of current-voltage characteristics for Au/Ni/GaN Schottky structure using I-V-T simulation

A. SADOUN^{1,*}, S. MANSOURI¹, M. CHELLALI¹, N. LAKHDAR², A. HIMA², Z. BENAMARA¹

¹Laboratoire de Micro-Electronique Appliquée, Université Djillali Liabes de Sidi Bel Abbès, BP 89, 22000 Sidi Bel Abbès, Algeria

²University of El Oued, Fac. Technology, Department of electrical engineering, 39000 El Oued, Algeria

In this work, we have presented a theoretical study of Au/Ni/GaN Schottky diode based on current-voltage (I-V) measurement for temperature range of 120 K to 400 K. The electrical parameters of Au/Ni/GaN, such as barrier height (Φ_b), ideality factor and series resistance have been calculated employing the conventional current-voltage (I-V), Cheung and Chattopadhyay method. Also, the variation of Gaussian distribution ($P(\Phi_b)$) as a function of barrier height (Φ_b) has been studied. Therefore, the modified ($(\ln(\frac{I_0}{T^2}) - \frac{q^2 \sigma_{s0}^2}{2kT^2}) = \ln(AA^*) - \frac{q\Phi_{B0}}{kT}$) vs. ($\frac{1}{kT}$) relation has been extracted from (I-V) characteristics, where the values of Φ_{B0} and A_{Simul}^* have been found in different temperature ranges. The obtained results have been compared to the existing experimental data and a good agreement was found.

Keywords: Schottky diode; Au/Ni/n-GaN; temperature effects; I-V characteristics; Cheung and Chattopadhyay method; SILVACO-TCAD

1. Introduction

The group III-V-N wide band gap semiconductors have attracted significant interest owing to the unique characteristics and their applications in microelectronic and optoelectronic devices operating in ultraviolet wavelength regions from 10 nm to 400 nm [1].

Gallium nitride is the most important semiconductor material for the development of microelectronic devices such as Schottky-barrier photodetectors, solar-blind Schottky photodiodes, metal-semiconductor (MS) field effect transistors (MES-FETs) and heterostructure field effect transistors (HFETs) [2]. The commonly used Schottky diode contains a contact between metal and semiconductor producing a Schottky barrier diode (MS). Many research groups investigated n-GaN-based metal-semiconductor by using different contact schemes for instance Ravinandan et al. [3] performed analysis of electronic parameters

and temperature-dependent properties of Pd/Au/n-GaN Schottky diodes in a wide temperature range of 90 K to 410 K. Reddy et al. [4] reported electrical properties and current transport mechanisms of Au/BaTiO₃/n-GaN that have been investigated by (I-V) and (C-V) measurements at room temperature. Yildirim et al. [5] studied the C-V and I-V characteristics of Ni/n-GaN Schottky diodes in different temperatures from 80 K to 400 K. Asha et al. [6] carried out an analysis of electronic parameters of V/p-type GaN Schottky junction at low temperatures in the range of 120 K to 280 K.

In this work, the I-V measurement of Au/Ni/GaN Schottky diodes in the temperature range of 120 K to 400 K is presented in order to demonstrate temperature effect on the structure performance. Different electrical characteristics of Au/Ni/GaN Schottky diodes, such as ideality factor n , barrier height and series resistance R_s were investigated by I-V, Cheung and Chattopadhyay method. These parameters were extracted using numerical simulator Atlas-Silvaco-Tcad software [7].

*E-mail: 3ali39@gmail.com

2. Modeling

In order to elucidate the effect of temperature on Au/Ni/GaN structure performance, modeling and simulation have been carried out using an ATLAS module of the SILVACO-TCAD software based on works of Dogan et al. [8]. ATLAS provides general capabilities of physically based 2D and 3D structures. It uses the drift-diffusion method to simulate optical, thermal and electrical behaviors of semiconductor devices. The electrical characteristics of the device can be obtained by solving the continuity model, Poisson equation and the transport model [9, 10].

The following equations and models were amongst the most important used here [10–12]:

- Band gap model;
- Mobility model;
- Shockley-Read-Hall model;
- Auger recombination;
- Impact ionisation;
- Thermionic emission;
- Universal Schottky tunnelling.

3. Result and discussions

3.1. Current-voltage (I-V) method

The effect of diode resistor can be modelled by a series combination of a diode and a resistor R_s through which the current flows. In addition, in case of an ideal diode, the value of the ideality factor n is equal to 1, while for the not ideal diode, the n value is higher than 1 ($n > 1$). In case of Schottky diode, assuming that the current is due to the thermionic emission TE, the relation between the applied forward bias and the current can be given by [4, 6, 8, 13]:

$$I = I_0 \exp\left(\frac{-qV}{kT}\right) \left[1 - \exp\left(\frac{q(V - IR)}{nkT}\right) \right] \quad (1)$$

Here, I_0 , n , k and T present the reverse saturation current, the ideality factor, the Boltzmann constant and the absolute temperature in Kelvin, respectively.

For the applied forward voltage ($V > 3kT/q$), the equation 1 can be written as [4]:

$$I = I_0 \exp\left(\frac{-qV}{kT}\right) \quad (2)$$

We can find the value of I_0 by plotting $\ln(I)$ versus V at $V = 0$ volts. Then, by replacing the calculated I_0 value in equation 2, we can find the Schottky barrier height Φ_b . The ideality factor n value can be extracted from the linear region of $\ln(I-V)$ curve (the straight line section of the curve):

$$I_0 = AT^2 A^* \exp\left(\frac{q\Phi_{b0}}{kT}\right) \quad (3)$$

where A is the rectifier contact area, Φ_b is the Schottky barrier height, The value of Φ_b can be deduced directly from I-V curves if the effective Richardson constant is known [13]. A^* is the Richardson constant ($A^* = 26.4 \text{ A/cm}^2 \text{ K}^2$ for n-GaN [4]).

Fig. 1 shows the current-voltage (I-V) characteristics of Au/Ni/GaN Schottky diode, simulated using Atlas-Silvaco-Tcad software at temperature range of 120 K to 400 K [14]. The obtained barrier height Φ_b and ideality factor n are shown in Table 1. The simulated ideality factor is found to be different than the experimental ideality factor by 0 and 0.085. The simulated barrier height is found to be different than the experimental barrier height by -0.016 and 0.008 in temperature range of 120 K to 400 K. According to what we found, we observed that the increase in temperature is accompanied by the decrease in the ideality factor and increase in the barrier height for the current-voltage method. These phenomena are due to the not pure thermionic emission current TE in the device [15, 16], because the charge carriers have not enough energy to cross the high barrier height at the low temperatures, but current transport is possible by lower parts of barrier height [17]. These variations of ideality factor and barrier height values suggest that Au/Ni/GaN is not an ideal diode and its charge transport mechanism is not just TE [20].

3.2. Cheung method

The Schottky barrier height Φ_b , the ideality factor n and the series resistance R_s can be calculated

Table 1. The obtained values of barrier height, ideality factor and series resistance for Au/Ni/GaN Schottky diode in 120 K < T < 400 K). (Exp. [8])

T [K]	I-V						G (I)				H (I)				Chattopadhyay	
	n	Φ_b [eV]		Rs [Ω]		n	Rs [Ω]		Φ_b [eV]		Rs [Ω]		n	Φ_b [eV]		
		Sim	Exp.	Sim	Exp.		Sim	Exp.	Sim	Exp.	Sim	Exp.				
120	2.471	2.556	0.300	0.301	769.23	-	3.100	-	781.31	866.02	0.218	0.264	744.12	882.81	2.475	0.334
140	2.250	2.273	0.330	0.332	739.64	-	2.532	-	702.32	724.42	0.300	0.299	730.20	733.53	2.252	0.327
160	2.040	2.085	0.365	0.368	581.39	-	2.301	-	580.00	598.55	0.342	0.340	620.00	607.80	2.159	0.351
180	1.880	1.925	0.400	0.403	446.42	-	2.223	-	510.20	480.10	0.381	0.374	501.32	489.18	2.079	0.383
200	1.801	1.823	0.410	0.419	385.80	-	2.153	-	430.53	409.10	0.400	0.388	451.32	425.20	1.851	0.398
220	1.700	1.727	0.450	0.454	380.12	-	1.952	-	365.19	361.25	0.410	0.403	370.20	360.06	1.818	0.432
240	1.635	1.649	0.481	0.475	333.33	-	1.703	-	320.10	331.13	0.422	0.439	340.13	338.26	1.757	0.457
260	1.570	1.573	0.500	0.497	294.11	-	1.683	-	280.12	298.58	0.436	0.433	332.53	289.57	1.672	0.476
280	1.520	1.520	0.520	0.526	284.09	-	1.643	-	275.83	310.92	0.483	0.481	310.31	317.32	1.658	0.505
300	1.473	1.476	0.550	0.549	279.50	-	1.592	-	273.03	292.95	0.491	0.488	296.82	291.70	1.594	0.529
320	1.420	1.419	0.579	0.582	271.32	-	1.531	-	268.52	287.68	0.520	0.519	290.53	289.02	1.592	0.549
340	1.382	1.384	0.610	0.614	268.12	-	1.486	-	260.50	286.90	0.540	0.543	290.23	285.11	1.582	0.590
360	1.331	1.340	0.653	0.650	260.31	-	1.442	-	257.32	282.97	0.581	0.572	280.35	278.23	1.517	0.615
380	1.320	1.321	0.701	0.685	257.73	-	1.403	-	249.32	274.82	0.601	0.599	260.21	266.28	1.490	0.624
400	1.280	1.289	0.713	0.721	250.00	-	1.370	-	230.62	267.30	0.673	0.638	245.32	247.57	1.464	0.646

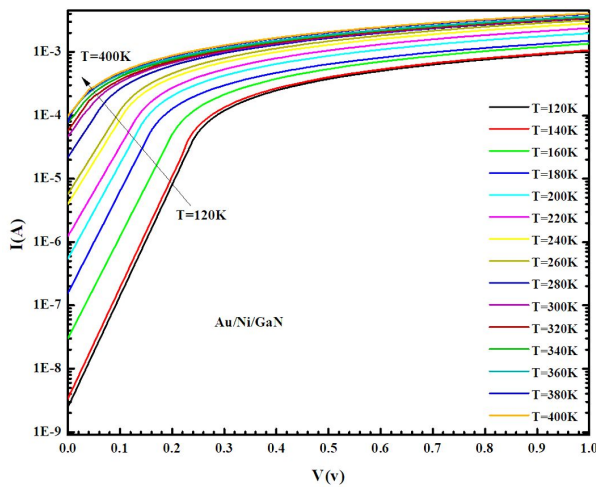


Fig. 1. The (I-V) characteristics of Au/Ni/GaN Schottky diode in the temperature range of 120 K to 400 K.

from the method developed by Cheung et al. [18]. In this method, the series resistance R_s and the ideality factor n are determined by the following equations:

$$G = \frac{\partial V}{\partial(\ln(I))} = \frac{nkT}{q} + I R_s \quad (4)$$

also, Schottky barrier height can be defined by Cheung relation [18]:

$$H(I) = V - \left(\frac{nkT}{q}\right) \ln\left(\frac{I}{AA^*T^2}\right) = n\Phi_{bn} + IR_s \quad (5)$$

Fig. 2 shows the obtained plots of $\frac{dV}{d(\ln(I))}$ and $H(I)$ as function of I for Au/Ni/GaN structure, at different temperatures.

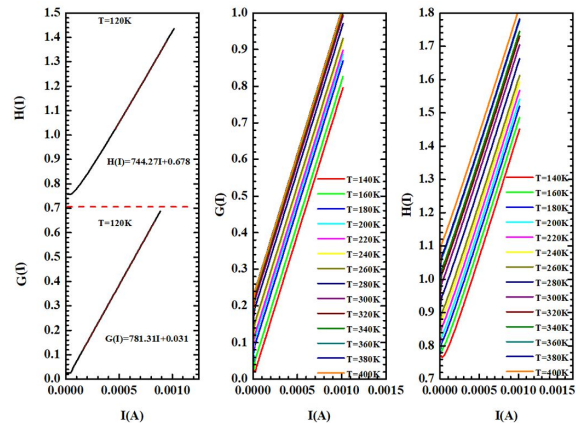


Fig. 2. The plots of $\frac{dV}{d(\ln(I))}$ and $H(I)$ as function of I for Au/Ni/GaN Schottky diode, at different temperatures.

The curve of $\frac{dV}{d(\ln(I))}$ is fitted to a straight line using equation 4. Both parameters, the ideality factor n and series resistance R_s have been extracted from the intercept and the slope of the line. We defined the function $H(I)$ by picking the value of n from equation 4 and substituted it in the equation 5. The plot of $H(I)$ as function of (I) at different temperatures is shown in Fig. 2. The two parameters i.e. the height of the Schottky barrier Φ_b , and the series resistance R_s can be determined by the Cheung method, where Φ_b value is given by y-axis intercept of $H(I)$ and R_s value is given by the slope. The obtained results for n , R_s and Φ_b , are shown in Table 1. The simulated series resistance R_s is found to be different from the experimental series resistance R_s by $-30.1 [\Omega]$ and $84.71 [\Omega]$ in temperature range of 120 K to 400 K. R_s values which were obtained from $G(I)$ and $H(I)$ vs. I plots were not so different from each other. These results confirm the consistency of Chung's function [19].

3.3. Chattopadhyay model

In addition, Chattopadhyay model can also be used to determinate the ideality factor and barrier height values of Schottky diode. In the present model, the barrier height Φ_b can be written as [20]:

$$\Phi_b = \Psi_s(J_C, V_C) + C_2 V_C + V_n - \frac{kT}{q} \quad (6)$$

where, $\Psi_s(J_C, V_C)$ present the critical surface potential, V_C is the critical voltage, V_n is the potential difference between the Fermi level and bottom of the conduction band and C_2 represents the parameter inverse of the diode ideality factor.

The critical surface potential value ($\Psi_s(J_C, V_C)$) can be determined by the following relation [20, 21]:

$$\Psi_s = \frac{kT}{q} \ln\left(\frac{AA^*}{I}\right) - v_n \quad (7)$$

and v_n parameter can be calculated from the following relation:

$$v_n = \frac{kT}{q} \ln\left(\frac{N_c}{N_d}\right) \quad (8)$$

where, N_c and N_d are the effective conduction band density of states and the carrier concentration, respectively. Using relation 8, we calculated V_n for different temperatures (120 K, 140 K, 160 K, 180 K, 200 K, 220 K, 240 K, 260 K, 280 K, 300 K, 320 K, 340 K, 360 K, 380 K and 400 K). The obtained values are 9.45×10^{-3} eV, 0.01 eV, 0.012 eV, 0.014 eV, 0.015 eV, 0.017 eV, 0.018 eV, 0.019 eV, 0.021 eV, 0.023 eV, 0.024 eV, 0.026 eV, 0.028 eV, 0.029 eV and 0.031 eV, respectively.

In order to determinate the inverse of the ideality factor C_2 , we used the following relation [20]:

$$C_2 = \frac{1}{n} = \left(\frac{d\Psi_s}{dV}\right)_{J_C, V_C} \quad (9)$$

Fig. 3 shows the surface potential vs. forward voltage (Ψ_s - V) of Au/Ni/GaN structure for different temperatures.

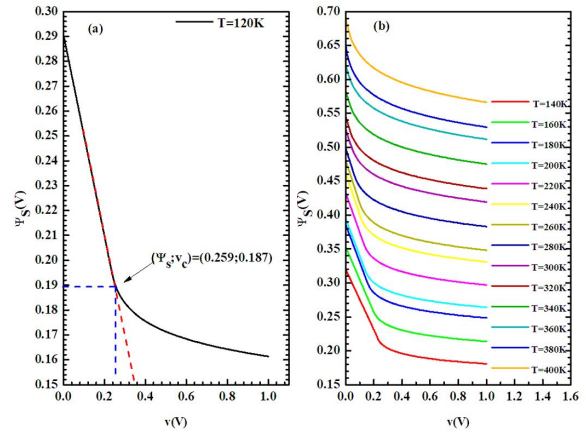


Fig. 3. Surface potential-forward voltage curves of the Au/Ni/GaN Schottky diode.

From Ψ_s - V behavior shown in Fig. 3, we remarked that the Ψ_s decreases with the increase in V while Ψ_s value increases with the temperature T . As shown in Fig. 3a, the critical values of V_C and Ψ_s have been extracted from the curve of Ψ_s and the slope has been marked with the red dashed line. The results of the critical values V_C and $\Psi_s(J_C, V_C)$, and barrier height Φ_b obtained using the Chattopadhyay model, are shown in Table 1.

The results, Φ_{b0} , n and R_s parameters for Au/Ni/GaN Schottky diode obtained using Cheung

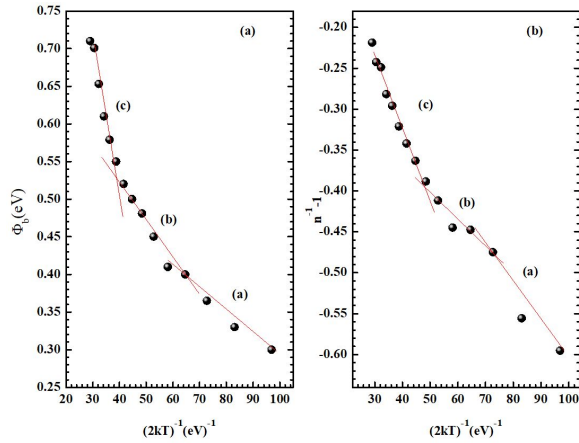


Fig. 4. (a) zero-bias apparent barrier height Φ_b , (b) ideality factor $(n^{-1} - 1)$ vs. $1/2kT$ plot for Au/Ni/GaN.

method and Chattopadhyay model are summarized in Table 1.

The results obtained by Chattopadhyay method show that an increase in temperature is accompanied by a decrease in the ideality factor and increase in the barrier height, which results from not pure thermionic emission current TE in the device [15, 16]. We have also observed that the Rs value decreases with increase in temperature. This reduction can be explained by the increase in free carrier concentration at high temperatures [8]. In addition, the Rs value obtained by four different methods is slightly different.

The differences in the barrier height values obtained by three methods may be due to the extraction of data from different regions of the forward-bias I-V plot [21, 22]. These results are in agreement with the studies performed by Ocak et al. [23].

3.4. Inhomogeneous barrier analysis

It is assumed that the mean Schottky barrier diode and the zero bias standard deviation are linearly dependent on Gaussian parameters, such as $\bar{\Phi}_b = \rho_2 v + \Phi_{b0}$ and standard deviation $\sigma_s = \sigma_{s0} + \rho_3 v$ [24], where ρ_2 and ρ_3 are voltage coefficients which may be dependent on T. They correspond to the voltage deformation of the barrier height distribution [25]. Fig. 4 shows the variation

of Φ_b and $n^{-1} - 1$ as function of $(2kT)^{-1}$. It was found that σ_s changes with temperature. The obtained results for σ_s are presented in Table 2.

Table 2. The calculated values of standard deviation σ_s , ρ_2 and ρ_3 in the temperature range of 120 K to 400 K.

T [K]	ρ_2 [V]	ρ_3 [V]	σ_s [eV]
Range(a)	0.132	-0.0048	0.054
Range(b)	0.260	-0.0028	0.090
Range(c)	0.016	-0.0076	0.130

In this model, the spatial distribution of the band bending, at the MS interface of Schottky contact can be approximated by Gaussian distribution $P(V_d)$ with a standard deviation, as described in equation 10 [26]:

$$P(V_d) = \frac{1}{\sigma_s \sqrt{2\pi}} e^{-\frac{(\bar{V}_d - V_d)^2}{2\sigma_s^2}} \quad (10)$$

where V_d represents the band bending and the Schottky barrier Φ_b :

$$\Phi_b = V_d + v + U \quad (11)$$

By taking V_d from equation 11 and replacing it in equation 10 the Gaussian distribution P can be written in function of Φ_b as:

$$P(\Phi_b) = \frac{1}{\sigma_s \sqrt{2\pi}} \exp \left[-\frac{(\Phi_{b0} - \bar{\Phi}_{b0})^2}{2\sigma_0^2} \right] \quad (12)$$

And around mean Schottky barrier (Φ_{b0}) the barrier distributions are normalized:

$$\int_{-\infty}^{\infty} P(V_d) dV_d = \int_{-\infty}^{\infty} P(\Phi_b) d\Phi_b = 1 \quad (13)$$

Fig. 5. shows the Gaussian distribution $P(\Phi_b)$ as function of barrier height Φ_b obtained from I-V method for Au/Ni/GaN, at T = 300 K.

3.5. Richardson constant A^*

Richardson constant can be calculated by two methods. In the first method conventional Richardson plot of reverse saturation current is made [8], as shown in the equation 14:

$$\ln \left(\frac{I_0}{T^2} \right) = \ln(AA^*) - \frac{q\Phi_b}{kT} \quad (14)$$

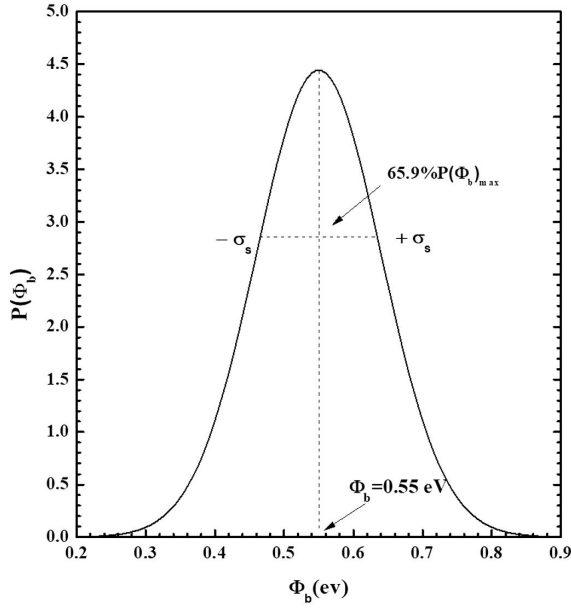


Fig. 5. Dependence of Gaussian distribution $P(\Phi_b)$ on barrier height Φ_b , obtained from I-V method for Au/Ni/GaN Schottky diode.

From the curve $\ln\left(\frac{I_0}{T^2}\right)$ vs. $\frac{1000}{T}$ shown in Fig. 6a we can get the activation energy E_a value from the slope and the Richardson constant A^* value at the y-axis intercept. We found the values of 0.1 eV and $1.07 \times 10^{-6} \text{ A}\cdot\text{cm}^{-2}\cdot\text{K}^{-2}$ respectively. These results are in good agreement with the results given in the literature [8].

In the second approach, we used an analytical potential fluctuation model employing different types of distribution function at the interface on the spatially inhomogeneous SBDs [28], Then, we have used equation 15:

$$\ln\left(\frac{I_0}{T^2}\right) - \left(\frac{q^2\sigma_s^2}{2kT^2}\right) = \ln(AA^*) - \frac{q\Phi_b}{kT} \quad (15)$$

From the plot of modified $\ln\left(\frac{I_0}{T^2}\right) - \left(\frac{q^2\sigma_s^2}{2kT^2}\right) = \ln(AA^*) - \frac{q\Phi_b}{kT}$ versus $\frac{1}{kT}$ shown in Fig. 6b, we can find that the modified Richardson plot has quite a good linearity over the whole temperature range. The Richardson constant values calculated using I-V method are collected in Table 3.

The value of Richardson constant A^* found in this work is $27.303 \text{ [A}\cdot\text{cm}^{-2}\cdot\text{K}^{-2}]$

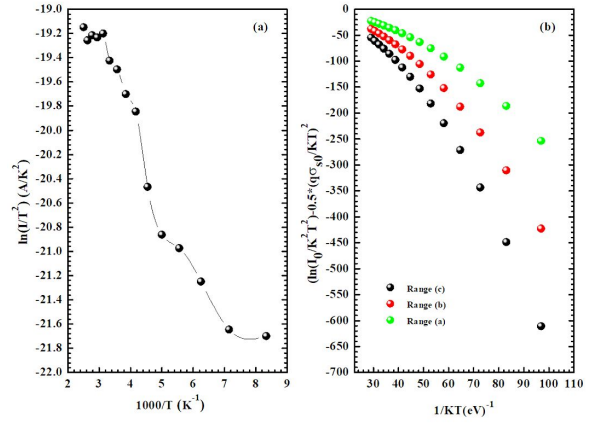


Fig. 6. (a) modified Richardson plots of $\ln\left(\frac{I_0}{T^2}\right)$ vs. $(1000/T)$ and (b) $\ln\left(\frac{I_0}{T^2}\right) - \left(\frac{q^2\sigma_s^2}{2kT^2}\right)$ vs. $(1/kT)$ for Au/Ni/n-GaN in the temperature range of 120 K to 400 K.

Table 3. The calculated values of the modified Richardson and Φ_b values.

	$A^* \text{ [A}\cdot\text{cm}^{-2}\cdot\text{K}^{-2}]$		$\Phi_b \text{ [eV]}$
	Present work	Other works [8]	Present work
Range (a)	21.321	10.199	0.52
Range (b)	27.303	26.293	0.86
Range (c)	36.705	34.750	1.25

which is very close to the theoretical value of $26.4 \text{ A}\cdot\text{cm}^{-2}\cdot\text{K}^{-2}$ for Au/Ni/GaN. This value is better than those obtained by Ravinandan et al. [3] $A^* = [20.43 \text{ A}\cdot\text{cm}^{-2}\cdot\text{K}^{-2}]$ in the range of $90 \text{ K} < T < 410, \text{ K}$, Shetty et al. [27] $A^* = 22.8 \text{ [A}\cdot\text{cm}^{-2}\cdot\text{K}^{-2}]$ in $150 \text{ K} < T < 370 \text{ K}$, Lakshmi [29] $A^* = 11.56$ in $120 \text{ K} < T < 270 \text{ K}$ and 23.48 in $270 < T < 390 \text{ [K}\cdot\text{A}\cdot\text{cm}^{-2}\cdot\text{K}^{-2}]$ and Elhaji et al. [30] $A^* = 8.73$ in $165 \text{ K} < T < 380 \text{ K}$, 47.88 in $380 \text{ K} < T < 480 \text{ [K}\cdot\text{A}\cdot\text{cm}^{-2}\cdot\text{K}^{-2}]$.

4. Conclusions

Current-voltage characteristics of an Au/Ni/n-GaN Schottky diode have been studied in temperature range of 120 K to 400 K. The ideality factor n and barrier height Φ_b values were calculated for various temperatures using thermionic emission TE theory. It is to note that the ideality

factor value decreases with increasing temperature and it diverges from the experimental data while the barrier height value increases with increasing temperature and it also diverges from the experimental data. These changes in ideality factor and barrier height values confirm that Au/Ni/n-GaN is not an ideal diode and charge transport mechanism is not based just on TE theory. The parameters, including R_s value, have also been calculated using Chung and Chattopadhyay method. In addition, the effective Richardson constant has been found to be 21.321 in the range of 300 K to 400 K, 27.303 in the range of 180 K to 300 K and 36.705 in the range of 120 K to 180 K. It can be noticed that the value of 27.303 $A^*(A \cdot cm^{-2} \cdot K^{-2})$ is very close to the theoretical value for Au/Ni/GaN.

References

- [1] LAKHDAR N., DJEFFAL F., DIBI Z., *AIP Conf. Proc.*, 1292 (2010), 173.
- [2] LAKHDAR N., DJEFFAL F., *Microelectron. Reliab.*, 56 (2012), 958.
- [3] RAVINANDAN M., RAO P.K., REDDY V.R., *Semicond. Sci. Tech.*, 24 (2009), 035004.
- [4] REDDY V.R., MANJUNATH V., JANARDHANAM V., KIL Y.-H., CHOI C.-J., *Electron. Mater.*, 43 (2014), 3499.
- [5] YILDIRIM N., EJDERHA K., TURUT A., *J. Appl. Phys.*, 108 (2010), 114506.
- [6] ASHA B., HARSHA C.S., PADMA R., REDDY V.R., *J. Electron. Mater.*, 47 (2018), 4140.
- [7] ATLAS D.S., *Silvaco International Software, Santa Clara, CA, USA*, 2005.
- [8] DOGAN H., ELAGOZ S., *Physica. E*, 63 (2014), 186.
- [9] HATHWAR R., DUTTA M., KOECK F.A., NEMANICH R.J., CHOWDHURY S., GOODNICK S.M., *J. Appl. Phys.*, 119 (2016), 225703.
- [10] FRITAH A., SAADOUNE A., DEHIMI L., ABAY B., *Philos. Mag.*, 96 (2016), 2009.
- [11] BERGMAN J., *Diam Relat. Mater.*, 6 (1997), 1324.
- [12] KHAN I.A., COOPER J.A., *IEEE T. Electron. Dev.*, 47 (2000), 269.
- [13] PADMA R., LAKSHMI B.P., REDDY M.S.P., REDDY V.R., *SuperlatticeMicrost.*, 56 (2013) 64.
- [14] AKKAL B., BENAMARA Z., BOUDISSA A., BOUIADJRA N.B., AMRANI M., BIDEUX L., GRUZZA B., *Mater. Sci. Eng. B-Adv.*, 55 (1998), 162.
- [15] JANARDHANAM V., KUMAR A.A., REDDY V.R., REDDY P.N., *J. Alloy. Compd.*, 485 (2009), 467.
- [16] SULLIVAN J., TUNG R., PINTO M., GRAHAM W., *J. Appl. Phys.*, 70 (1991), 7403.
- [17] AYDOGAN S., SAGLAM M., TÜRÜT A., *Appl Surf Sci.*, 250 (2005), 43.
- [18] CHEUNG S., CHEUNG N., *Appl. Phys. Lett.*, 49 (1986), 85.
- [19] KOCYIGIT A., ORAK I., ÇALDIRAN Z., TURUT A., *J. Mater Sci-Mater El.*, 28 (2017), 17177.
- [20] CHATTOPADHYAY P., *Solid State Electron.*, 38 (1995), 739.
- [21] KARATAS S., YILDIRIM N., TÜRÜT A., *SuperlatticeMicrost.*, 64 (2013), 483.
- [22] GÜLLÜ Ö., AYDOGAN S., TÜRÜT A., *Microelectron. Eng.*, 85 (2008), 1647.
- [23] OCAK Y., KULAKCI M., KILIÇOĞLU T., TURAN R., AKKILIÇ K., *Synthetic Met.*, 159 (2009), 1603.
- [24] DOGAN H., YILDIRIM N., ORAK I., ELAGÖZ S., TURUT A., *Physica B.*, 457 (2015), 48.
- [25] ZHU S., DETAVERNIER C., VAN MEIRHAEGHE R., CARDON F., RU G.-P., QU X.-P., LI B.-Z., *Solid State Electron.*, 44 (2000), 1807.
- [26] WERNER J.H., GÜTTLER H.H., *J. Appl. Phys.*, 69 (1991), 1522.
- [27] SHETTY A., ROUL B., MUKUNDAN S., MOHAN L., CHANDAN G., VINOY K., KRUPANIDHI S., *AIP Adv.*, 5 (2015), 097103.
- [28] ZEGHDAR K., DEHIMI L., SAADOUNE A., SENGOUGA N., *J. Semicond.*, 36 (2015), 124002.
- [29] LAKSHMI B.P., REDDY M.S.P., KUMAR A.A., REDDY V.R., *Curr. Appl. Phys.*, 12 (2012), 765.
- [30] ELHAJI A., EVANS-FREEMAN J., EL-NAHASS M., KAPPERS M., HUMPHRIES C., *Mat. Sci. Semicon. Proc.*, 17 (2014), 94.

Received 2019-01-05

Accepted 2019-04-25